

## Temperature dependence of the tunneling spectrum near a vortex core

L. L. Daemen and A. W. Overhauser

*Department of Physics, Purdue University, West Lafayette, Indiana 47907*

(Received 15 May 1989)

We propose a simple model to account for the anomaly observed in the tunneling conductance at a vortex core in NbSe<sub>2</sub> by Hess *et al.* The sharp peak occurring at low bias is attributed to self-energy corrections of the normal electrons in the core caused by their coupling to superconducting excitations outside the core. The temperature dependence of the tunneling spectrum is calculated, and the low-bias peak is found to increase significantly at reduced temperature. However, the width hardly changes, but the dips on each side of the low-bias peak become more pronounced. Finally, we show that an appropriate (spatially dependent) admixture of the tunneling spectrum at the vortex center with the spectrum two coherence lengths away explains the position dependence of the tunneling conductance.

### I. INTRODUCTION

Various attempts<sup>1-3</sup> have been made in the past to calculate the local density of states near a vortex in a type-II superconductor. The conclusion reached was that the density of states near the Fermi energy must either be constant (equal to the normal-state value) or perhaps have a reduced value near the center of a vortex. For a long time such measurements have been out of reach of conventional tunneling spectroscopy, but the advent of scanning tunneling microscopy now makes it possible to probe directly the *local* density of states and to test the theoretical predictions.

A recent scanning tunneling microscope (STM) investigation by Hess *et al.*<sup>4</sup> of the density of states at the center of a vortex core in NbSe<sub>2</sub> revealed an unexpected increase of the tunneling conductance at low bias, in contradiction to the theoretical calculations. Their data are shown in Fig. 1 for three STM locations. The zero-bias peak in curve *a* of Fig. 1 rises 100% above the asymptotic value, and the dips on either side are about 25%. The spectrum found 2000 Å from the vortex, curve *c* of Fig. 1, was the same as the spectrum found in zero field (when there is no vortex lattice present).

In a previous publication<sup>5</sup> we proposed a simple explanation of the effect observed by Hess *et al.*, and were able to fit their data rather well. The purpose of this paper is threefold. First, we want to justify in more detail the theoretical approach of Ref. 5 which, because of space limitations, was presented succinctly. Second, we present new results on the temperature dependence of the tunneling conductance at a vortex core. Finally, we suggest a simple way to account for the position dependence of the tunneling spectrum for STM locations within two coherence lengths of the central axis of a vortex.

### II. THEORY

#### A. Theoretical model

Before coming to grips with the problem of calculating the density of states at the center of a vortex core, we

shall describe briefly the physical mechanism which we think is responsible for the enhancement of the low-bias conductance in the experiment of Hess *et al.* It should be emphasized at this point that although the transition from “normal” (at the center of the vortex core) to “superconducting” behavior (outside the vortex) is a gradual one; its relative sharpness allows us to distinguish between “normal” electrons and “superconducting” excitations. Therefore we can divide our basis functions into these localized within the vortex (which we assume to be a cylinder of radius  $R \approx \xi_0$ , the coherence length) and those outside. Because of the overlap between these two sets of wave functions, there will be a (mean) hopping matrix element  $t$  from inside to outside; i.e., there is a finite probability for a normal electron to escape from the vortex by tunneling into the superconducting region outside the vortex. This coupling of the normal states to the superconducting excitations is not only responsible for their “decay,” but also, and more importantly here, it is responsible for shifting their energy by a small amount,

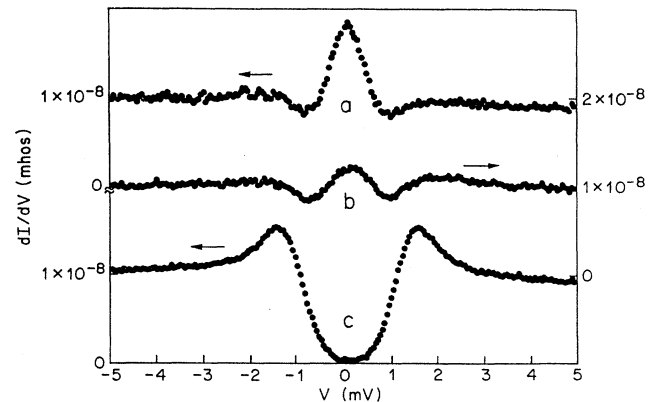


FIG. 1. STM tunneling conductance for NbSe<sub>2</sub> at 1.85 K and  $H=0.02$  T. Curve *a* is the spectrum at the center of the vortex; curve (b) is 75 Å away from the vortex; curve *c* is 2000 Å away from the vortex. The zero of each successive curve has been shifted up by one-quarter of the vertical scale for clarity. The data are from Hess *et al.* (Ref. 4). For NbSe<sub>2</sub>,  $\xi_0 = 77$  Å.

thereby modifying their density of states. This situation is reminiscent of several important problems in physics, such as, for instance,  $\alpha$  decay, autoionization of many-electron atoms, spontaneous emission of a photon by excited atomic or nuclear levels, etc. The crucial point, common to all these problems, is that once a quantum state is coupled by a perturbation to a continuum of states, it acquires a finite lifetime *and its energy is shifted*. This effect was initially discovered by Weisskopf and Wigner.<sup>6</sup> (A more accessible treatment can be found in Ref. 7.)

### B. Decay rate

Let us now consider the quantum-mechanical problem of a discrete state coupled by a time-independent perturbation  $W$  to a continuum of states. The Hamiltonian of the unperturbed system is designated by  $H_0$ . Its spectrum includes a discrete state  $|\phi\rangle$  with energy  $w$ :  $H_0|\phi\rangle = w|\phi\rangle$ , and a continuum of states  $|\alpha\rangle$  with energies  $\epsilon$ :  $H_0|\alpha\rangle = \epsilon|\alpha\rangle$ . In general, the energy of the discrete state falls within the energy range of the continuum. It is further assumed that these states form a complete set and that the perturbation  $W$  couples *only* the discrete state to the continuum, i.e., the matrix elements  $\langle\phi|W|\phi\rangle$ ,  $\langle\alpha|W|\alpha\rangle$ , and  $\langle\alpha'|W|\alpha\rangle$  are identically zero. Finally, we designate the density of states in the continuum which are coupled to  $|\phi\rangle$  by  $N_s(\epsilon)$ .

It is of course well known that the decay rate is given by Fermi's "golden rule":

$$\gamma(w) = \frac{2\pi}{\hbar} t^2 N_s(w), \quad (1)$$

where  $t$  is the hopping matrix element from inside to outside the core. In order to evaluate this matrix element, we have to elucidate somewhat its physical origin. This is most conveniently done by recalling the superlattice representation,<sup>8</sup> the basis functions of which are specified by a superlattice cell  $\mathbf{L}_i$  and a coarse-grained momentum  $\mathbf{K}_i$ . The size of the superlattice cell can be chosen to have any value between an atomic cell and the entire crystal, so representations having any degree of localization between the Wannier limit and the Bloch limit are possible. It can be shown<sup>8</sup> that a consequence of having a semilocalized basis is that the kinetic energy operator acquires off-diagonal matrix elements between basis states in neighboring cells. Consider then a metal in the normal state to be divided into a cylinder of radius  $\xi_0$  and the entire region outside. (Below the transition temperature  $T_c$  the cylinder will be identified with a vortex core.) Above  $T_c$  the hopping matrix element  $t$  from inside the cylinder to outside can be determined by requiring that the golden rule transition rate

$$\frac{1}{\tau} = \frac{2\pi}{\hbar} t^2 N_0 \quad (2)$$

be consistent with the mean time  $\tau \simeq \xi_0/v_F$  needed for an electron traveling at the Fermi velocity  $v_F$  to escape from the cylinder.  $N_0$  is the density of normal states outside the cylinder for  $T > T_c$  which are connected to those inside by  $t$ . Since the mean distance to the boundary of a

unit cylinder (along a fixed direction perpendicular to the axis) and from an arbitrary point inside is  $8/3\pi$ , we take  $\tau$  to be

$$\tau = 8\xi_0/3\pi v_F. \quad (3)$$

Now the coherence length is given by<sup>9</sup>

$$\xi_0 = \hbar v_F / \pi \Delta, \quad (4)$$

where  $\Delta$  is the superconducting gap parameter at  $T=0$ . Combining Eqs. (2)–(4), we find

$$t^2 = \frac{3\pi\Delta}{16N_0}. \quad (5)$$

It is noteworthy that  $\xi_0$  and  $v_F$  have dropped out and that  $\Delta$ , which sets the energy scale, remains. Now in a weak coupling superconductor the transition matrix element from normal electron states to superconducting excitations does not change.<sup>10</sup> Accordingly, the decay rate (1) for normal electrons in a vortex core is completely specified by the matrix element  $t$ , from Eq. (5), provided  $N_s(w)$  is the density of superconducting excitations outside the core. We will discuss  $N_s(w)$  in detail in Sec. III.

### C. Energy shift

Not only does the coupling with a continuum make a discrete state unstable, it also shifts its energy from  $w$  to  $E$  by an amount  $\Sigma(E)$ :

$$E = w + \Sigma(E). \quad (6)$$

The fact that a discrete state is unstable is sometimes accounted for by assigning a complex "energy" to it:

$$E = i\frac{1}{2}\hbar\gamma(E) = w + \Sigma(E) - i\frac{1}{2}\hbar\gamma(E) \equiv w + \sigma(E), \quad (7)$$

where we have introduced the so-called self-energy  $\sigma$  with the usual meaning attached to it, i.e., the real part of  $\sigma$  is the "true" energy shift while its imaginary part is proportional to its decay rate. A simple, approximate expression for  $\Sigma$  was obtained by Weisskopf and Wigner,<sup>6,7</sup> who showed that the energy shift  $\Sigma$  can be calculated by using time-independent perturbation theory. Their expression for  $\Sigma$ , however, is too crude for our purpose here. Its use leads to a correction in the density of states which qualitatively resembles the experimental result, but no quantitative fit can be obtained. So it is crucial to calculate the energy shift  $\Sigma$  with the greatest possible accuracy.

In order to motivate an accurate theory for  $\Sigma(E)$  we consider a set of discrete states  $\{|\alpha_i\rangle\}$ . The case of interest here is a continuum of states, but for the sake of simplicity, in order to avoid cumbersome notations, we illustrate our point on a discrete set of states; the conclusion remains unchanged for a continuum, and we suppose that we have diagonalized the Hamiltonian in the portion of Hilbert space spanned by this set of states. If we now include one more state, coupled in general to all the states  $\{|\alpha_i\rangle\}$  by a time-independent perturbation, then in order to determine the energy correction to each state, one has to solve the following secular equation:

$$\det \begin{pmatrix} E-w & W_1 & W_2 & \cdots & W_n \\ W_1^* & E-\varepsilon_1 & 0 & \cdots & 0 \\ W_2^* & 0 & E-\varepsilon_2 & \cdots & 0 \\ \vdots & \vdots & \vdots & \ddots & \vdots \\ W_n^* & 0 & 0 & \cdots & E-\varepsilon_n \end{pmatrix} = 0. \quad (8)$$

The determinant is readily evaluated:

$$(E-w) \prod_{i=1}^n (E-\varepsilon_i) - \sum_{i=1}^n |W_i|^2 \prod_{j \neq i} (E-\varepsilon_j) = 0. \quad (9)$$

After dividing this equation by the first product which appears, we can rewrite Eq. (9) in the following way:

$$E = w + \sum_{i=1}^n \frac{|W_i|^2}{E-\varepsilon_i}, \quad (10)$$

and this is nothing else but the result one would have obtained by using the first term only of a Brillouin-Wigner perturbation expansion.<sup>11</sup> However, Eq. (10) is the *exact* result for the problem considered here.<sup>12</sup> This important result being established, let us turn our attention to the calculation of the energy shift  $\Sigma(E)$  caused by a continuum of  $\varepsilon$ 's

Crudely speaking, the states in the continuum can be divided into a set of states contributing essentially to the finite lifetime of the discrete state and a set of states contributing essentially to the energy shift.<sup>7</sup> The first set of states corresponds to the continuum states having an energy close to the energy of the discrete level; the second set to all those remaining. The decay of the discrete state to the first set of states must be blocked, otherwise an exact solution for the wave function having original energy  $w$  will consist almost entirely of components from the (outside) continuum. Our interest is only in the corrected energy  $E$  of this level in so far as it has not decayed into the continuum. However, a sharp division, as in Fig. 2(a), between states contributing to the decay (and to be treated by time-dependent perturbation theory) and states contributing to the energy shift  $\Sigma(E)$ , and to be treated by a time-independent method, does not seem appropriate.

There is, however, a simple way to determine to what extent a state in the continuum "contributes" to the decay of a discrete state. Indeed, we know that if we wait long enough, the discrete state decays and the distribution in energy of the final states is proportional to a Lorentzian centered on the shifted energy  $E$ :

$$\frac{1}{(E-\varepsilon)^2 + (\hbar\gamma/2)^2}, \quad (11)$$

shown in Fig. 2(b). Therefore, when calculating  $\Sigma$  from the second term of Eq. (10), we should weigh the contribution of each state in the continuum to the extent that it does not participate in the decay. Accordingly,

$$\Sigma = \int_{-\infty}^{+\infty} d\varepsilon \frac{t^2 N_s(\varepsilon)}{E-\varepsilon} \left[ 1 - \frac{(\hbar\gamma/2)^2}{(E-\varepsilon)^2 + (\hbar\gamma/2)^2} \right]. \quad (12)$$

Notice that we have normalized the Lorentzian so that the contribution of the state with energy  $\varepsilon = E$  is exactly

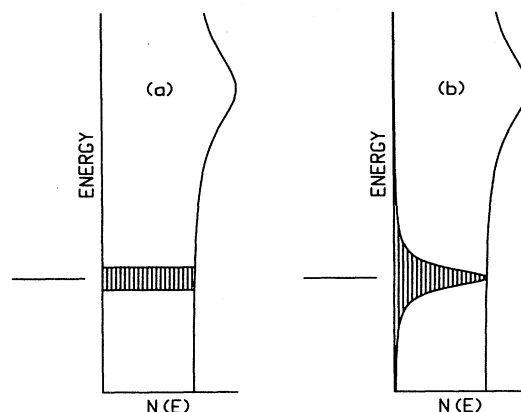


FIG. 2. A discrete state is shown adjacent to the continuum density of states with which it interacts and into which it can decay. The shaded area corresponds to the states involved in the decay and which do not contribute to the energy shift. (a) A naive "rectangular" set of states which must be deleted from the eigenvalue equation (10), to close off decay. (b) A refined "Lorentzian" set of states which are "closed" in proportion to their contribution to the decay process from time-dependent perturbation theory.

zero, which is required to completely block the decay. Equation (12) can be rewritten in a slightly different way:

$$\Sigma(E) = \int_{-\infty}^{+\infty} d\varepsilon \frac{t^2 N_s(\varepsilon)(E-\varepsilon)}{(E-\varepsilon)^2 + (\hbar\gamma/2)^2}, \quad (13)$$

or

$$\Sigma(E) = \text{Re} \int_{-\infty}^{+\infty} d\varepsilon \frac{t^2 N_s(\varepsilon)}{E-\varepsilon - i\hbar\gamma/2}. \quad (14)$$

The result for  $\Sigma(E)$ , given by Eq. (14), is new to us. It would be of interest to see whether an alternative derivation can be found using the formalism developed in collision theory for the description of decaying states.<sup>13</sup> Equation (14) resembles the first term of a Brillouin-Wigner expansion, but the resemblance is merely a mnemonic convenience. (Brillouin-Wigner perturbation theory cannot handle complex energies.) Moreover, Eq. (14) is an exact expression for  $E$ , given the unblocked portion of the continuum used in Eq. (12) and shown in Fig. 2(b), and is not merely the first term of an expansion.

#### D. Density of states

The final step consists in calculating the core electron density of states  $N(E)$ . This quantity is related to the energy shift  $\Sigma(E)$  as follows. If  $Z$  is the number of states with energy less than  $w$ , where  $w$  is, as already defined above, the energy of a core electron before perturbation, then

$$N_c \equiv \frac{dZ}{dw}. \quad (15)$$

Now,  $Z(E)$  is the number of states with energy less than  $E$ , so the density of states after perturbation is

$$N(E) \equiv \frac{dZ(E)}{dE} = N_c \left[ \frac{dE}{ew} \right]^{-1}. \quad (16)$$

Now, by virtue of Eq. (6), one finds

$$\frac{dE}{dw} = 1 + \frac{d\Sigma}{dE} \frac{dE}{dw}. \quad (17)$$

Upon solving this equation for  $dE/dw$  and after substitution of the result in Eq. (16), the density of states  $N(E)$  becomes<sup>14</sup>

$$N(E) = N_c \left[ 1 - \frac{d\Sigma}{dE} \right], \quad (18)$$

which is easily evaluated once  $\Sigma(E)$  is known.

### III. TUNNELING CONDUCTANCE

The density of states  $N(E)$  can be calculated numerically from Eqs. (13) and (18). On conversion to dimensionless variables,  $x = E/\Delta$ ,  $y = \varepsilon/\Delta$ , Eq. (13) becomes

$$\frac{\Sigma(x)}{\Delta} = \frac{3\pi}{16} \int_{-\infty}^{+\infty} \frac{(x-y)g(y)dy}{(x-y)^2 + (3\pi^2/16)^2 g^2(x)}, \quad (19)$$

where

$$g(E) \equiv \frac{N_s(E)}{N_c}. \quad (20)$$

We must now find an analytic expression for  $g(x)$  which fits the experimental spectrum far from the vortex, curve *c* of Fig. 1, and which conserves the total number of states. A possible choice is

$$g(x) = \frac{2ax^2/\pi}{(x^2-1)^2 + a^2x^2} + \frac{1}{1 + \exp[b(1-x)]} + \frac{1}{1 + \exp[b(1+x)]}. \quad (21)$$

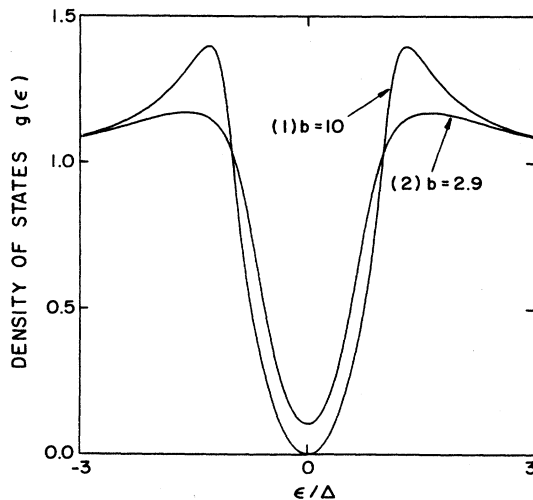


FIG. 3. Density of states of the superconducting excitations,  $g(x) = N_s(E)/N_0$ , modeled by Eq. (21) for  $a=1.2$  and two values of  $b$ . The curve for  $b=10$  models the observed spectrum, curve *c* of Fig. 1, 2000 Å from the vortex. The curve for  $b=2.9$  models the expected spectrum just outside the vortex core.

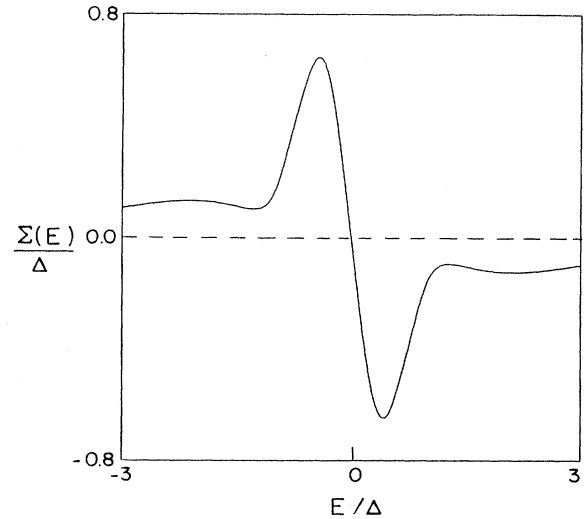


FIG. 4. Energy shift  $\Sigma(E)$  for the electrons in a vortex core, calculated from Eq. (13) using the density of superconducting excitations given by curve (1) of Fig. 3.

$g(x)$  is displayed in Fig. 3, curve (1) for  $a=1.2$  and  $b=10$ , and should be compared with Fig. 1, curve *c*. The energy shift  $\Sigma$  calculated from Eq. (13) is shown in Fig. 4. Notice that states above  $E_F$  ( $E > 0$ ), are displaced downwards whereas states below  $E_F$  are displaced upwards.

The density of states, obtained from Eq. (18), is shown by curve (1) of Fig. 5. The peak at  $E=0$  is obviously the consequence of the "squeezing" action of  $\Sigma(E)$  just mentioned. Comparison of this curve with curve *a* of Fig. 1 shows that the qualitative features of the data are reproduced but are somewhat exaggerated. However, the tun-

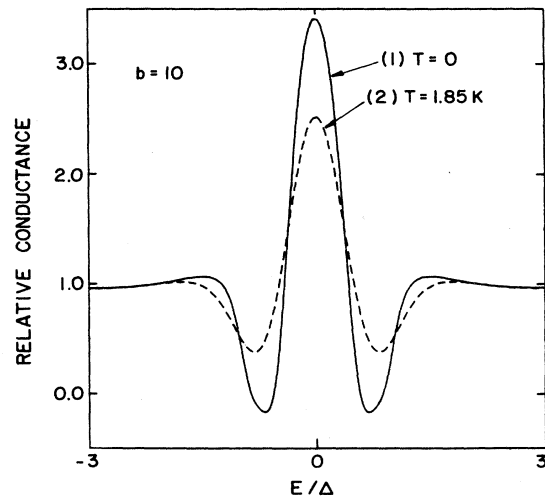


FIG. 5. The solid curve is the relative density of states for (normal) electrons in a vortex core obtained from Eq. (18) by differentiating  $\Sigma(E)$  shown in Fig. 4. The dashed curve is the relative conductance at  $T=1.85$  K obtained by convoluting the solid curve with the Fermi-Dirac factors according to Eq. (25).

neling conductance is proportional to  $N(E)$  only at  $T=0$ . Finite temperature effects, to be described below, lead to curve (2) for  $T=1.85$  K (the measurement temperature). No new parameters are involved here, since  $a$  and  $b$  of Eq. (21) were used to fit curve  $c$  of Fig. 1. Therefore the zero-bias anomaly predicted without benefit from adjustable parameters agrees very well with experiment and is too large by only 50%.

The superconducting spectrum we used for  $g(x)$  was based on the experimental tunneling spectrum far away from the vortex core and, consequently, does not take account of the fact that the superconducting excitations accessible to the normal electrons (inside the core) are located just outside the core where critical currents circulate. Now it is known that superconducting excitations in a region carrying a critical current are gapless.<sup>15</sup> Accordingly, the parameter  $b$  in Eq. (21) can be reduced so that there will be a finite density of states at  $\varepsilon=0$ . If we take  $b=2.9$ , keeping  $a=1.2$ , the density of excitations just outside the core is modeled by curve (2) of Fig. 3. Note that  $g(0)$  is now  $\approx 0.1$ . The relative density of states inside the core [calculated from Eqs. (13) and (18)] is now shown by curve (1) of Fig. 6, which would also be the relative conductance at  $T=0$ . At  $T=1.85$  K the theoretical conductance becomes the dashed curve, (2) of Fig. 6. It is essentially a perfect fit to the data, curve  $a$  of Fig. 1, and reveals the dips on either side of the zero-bias peak and also the small shoulders near  $E=\pm 1.5\Delta$ . Of course the value of  $b$  was chosen to achieve this success.

Notice finally that if superconductivity disappears, i.e., if  $g(\varepsilon)$  becomes a constant, the energy shift for electrons in the core goes to zero. Thereupon the density of states  $N(E)$  becomes constant (and equal to  $N_c$ ).

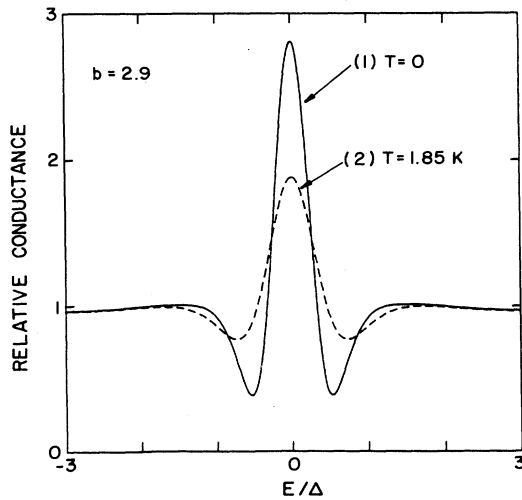


FIG. 6. The solid curve is the relative density of states for (normal) electrons based on  $g(x)$ , Eq. (21) with  $a=1.2$  and  $b=2.9$ , i.e., the superconducting excitations spectrum shown in curve (2) of Fig. 3. The dashed curve is the relative conductance at  $T=1.85$  K obtained by convoluting the solid curve with the Fermi-Dirac factors according to Eq. (25). The dashed curve matches the data of curve  $a$  of Fig. 1a.

#### IV. TEMPERATURE DEPENDENCE

We now turn to the temperature dependence of the tunneling conductance. Some results from this section have already been shown in Figs. 5 and 6. We first emphasize that we shall confine our attention to temperatures  $T < 0.3T_c$ , so that variations in the gap parameter  $\Delta(T)$  can be ignored. Since  $T_c \approx 7.2$  K for NbSe<sub>2</sub>, the published data<sup>4</sup> (taken at 1.85 K) allows this simplification.

The first remark is to note that there is no temperature dependence in the renormalization of  $N(E)$ , for states inside the core, caused by the hopping matrix elements  $t$ , which are nondynamic, i.e., independent of time. (It is well known<sup>16</sup> that dynamic perturbations, e.g., electron-phonon interactions, cause a temperature-dependent contribution to the self-energy.) The reason for the temperature independence in the present case is easy to understand. The energy shift of a particular state  $\varepsilon_0$  in an  $N+1$  particle system is the total shift with that state occupied minus the total shift (of the  $N$  particle system) with that state empty. Consequently,

$$\Delta\varepsilon_0 = \sum_i \frac{t_{0i}^2 [1 - f(\varepsilon_i)]}{\varepsilon_0 - \varepsilon_i} - \sum_i \frac{t_{0i}^2 f(\varepsilon_i)}{\varepsilon_i - \varepsilon_0}, \quad (22)$$

where  $f(\varepsilon_i)$  is the Fermi-Dirac factor. It is evident that the terms involving  $f(\varepsilon_i)$  in Eq. (22) cancel.

The tunneling conductance between a STM tip and the electronic states near a vortex will nevertheless be temperature dependent because of the structure in  $N(E)$ . The relative conductance is<sup>17</sup>

$$g(V, T) = \int_{-\infty}^{+\infty} \frac{N(E)}{N_c} \left[ -\frac{\partial}{\partial E} f(E + eV) \right] dE. \quad (23)$$

Since

$$-\frac{\partial f(E)}{\partial E} = f(E)[1 - f(E)], \quad (24)$$

the relative conductance becomes

$$g(V, T) = \int_{-\infty}^{+\infty} \frac{N(E)}{N_c} f(E + eV)[1 - f(E + eV)] \frac{dE}{k_B T}. \quad (25)$$

It is evident that the relative differential conductance is just the convolution of the relative density of states with  $f(1-f)$ .  $g(V, T)$  is shown in Fig. 7 for four temperatures. The zero-bias peak grows with decreasing temperature and the dips on either side become more pronounced.

The temperature dependence of the conductance is certainly interesting to study, first because it can be determined experimentally and second because it provides a crucial test for our model, or any other model designed to account for this type of anomaly. (It is of course necessary to experimentally relocate the STM at the vortex center with each change in temperature.) We conclude this section by stressing that, in order for the measurements to be reliable, one has to make sure that the tunneling conductance is independent of the current so that any observed temperature dependence cannot be attributed to heating effects at the STM tip.

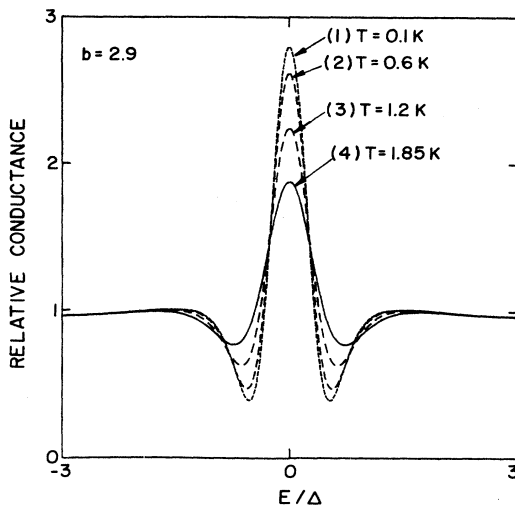


FIG. 7. Theoretical relative conductance curves for four temperatures.

### V. POSITION DEPENDENCE

Attention has so far been focused on the voltage dependence of the tunneling conductance, particularly when a STM is located at the center of a vortex. We have assumed that for this location electrons in the STM tip tunnel primarily to the normal electron states inside the vortex core of radius  $R$ . For STM locations just outside the core, say at  $r=2R$ , the electrons in the STM tip will tunnel primarily to the superconducting excitations, which have a distribution given by curve (2) of Fig. 3 (on account of the critical currents which flow in this region and create the fluxoid).

If a STM tip is moved continuously from  $r=0$  to  $r=2R$ , the tunneling conductance will transform gradually from  $g_c(V)$ , given by curve (2) of Fig. 6 to  $g_s(V)$ , given by curve (2), Fig. 3, since the only fermion-like states accessible near a vortex are the two species already described. Accordingly the  $r$  dependence of the conductance  $g(V, r)$  will be a statistically weighted sum of the two limiting functions:

$$g(V, r) = \eta(r)g_s(V) + [1 - \eta(r)]g_c(V). \quad (26)$$

$\eta(r)$  is a continuous weight function, which varies from (essentially) nil at  $r=0$  to unity near  $r=2R$ , and is the probability that a tunneling event between the superconductor and the STM tip involves transfer to (or from) a superconducting excitation. The spatial dependence of  $\eta(r)$  is illustrated schematically in Fig. 8. It seems reasonable to assume that  $\eta(r)$  is a smooth monotonic function, as shown. The number of electron states within a vortex core per  $\mu$  of length (for  $\text{NbSe}_2$ ) and within  $\pm\Delta$  of the Fermi energy is  $\approx 2 \times 10^4$ . Any attempt to calculate  $\eta(r)$  microscopically would require knowledge of the wave functions of all these states (in the core) as well as of the excitations outside. The smoothness of  $\eta(r)$ , which we have assumed, seems likely because nodes of individual states would be averaged out by the extensive summation.

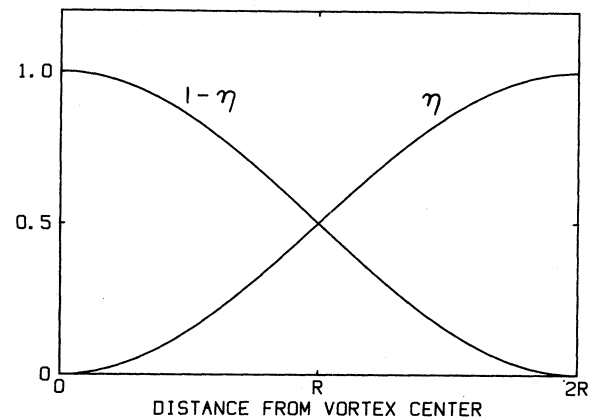


FIG. 8. Schematic behavior of the weight function  $\eta(r)$  and  $1-\eta(r)$  which are respectively, the tunneling of the weight function  $\eta(r)$  and  $1-\eta(r)$  which are, respectively, the tunneling fraction to superconducting excitations or to normal electrons inside the core (of radius  $R$ ).

It seems appropriate to define the radius  $R$  of a vortex core to be that value of  $r$  for which  $\eta(R)=0.5$ . Accordingly for a STM located at  $R$ , half of the tunneling events involve the normal electrons inside the core, and the other half involve the superconducting excitations outside. Such a definition allows  $R$  to be measured experimentally, once the relative conductances  $g_s(V)$  and  $g_c(V)$  have been determined. In Fig. 9 we show  $g(V, r)$ , calculated from Eq. (26), for three values of  $\eta$ . The STM location  $r$  which exhibits the conductance shown for  $\eta=0.5$  determines  $R$ . The conductance curve for  $\eta=0.38$  in Fig. 9 has been shown because it is an exact fit to the data of Fig. 1(b).

Figure 10 is a simulated plot of a zero-bias STM position scan along a straight line passing through a vortex

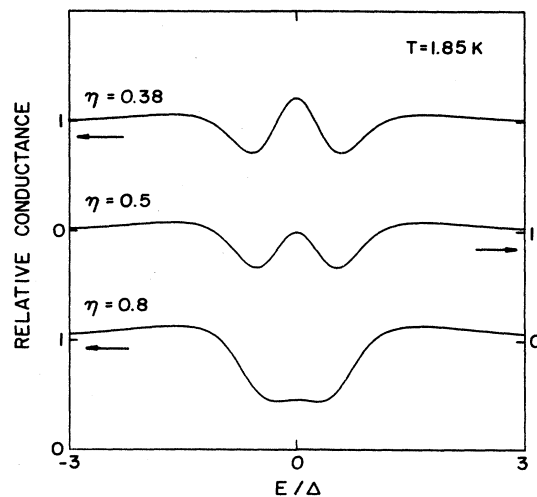


FIG. 9. Relative tunneling conductance for three values of the weight function  $\eta$ . The curve for  $\eta=0.38$  fits the experimental data shown in curve *b* of Fig. 1.

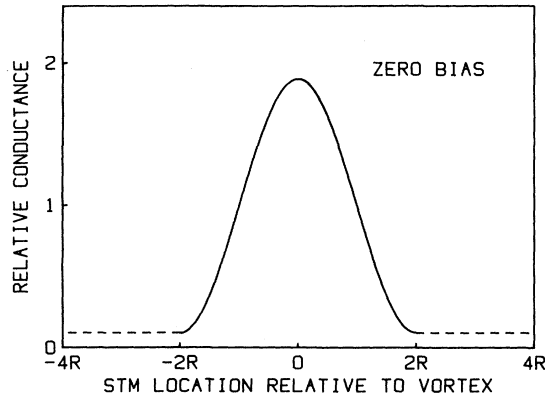


FIG. 10. Zero-bias conductance along a STM scan line through the center of a vortex (having a core of radius  $R$ ). The dashed extensions approach zero at large distance from the vortex center.

center. The curve (between  $-2R$  and  $2R$ ) was calculated with  $\eta(r) = \sin^2(\pi r/4R)$ , also used in Fig. 8. This heuristic choice has a half-width (at half maximum) equal to  $R$ . The "note added" in Ref. 4 describes a careful STM scan at zero bias and reports that the half-width was  $77 \pm 5 \text{ \AA}$ . It is noteworthy that the half-width of such a scan, which we suggest be taken as the phenomenological definition of  $R$ , the vortex core radius, agrees with the coherence length  $\xi_0 = 77 \text{ \AA}$  for  $\text{NbSe}_2$ .<sup>18</sup> The dashed extensions of the curve in Fig. 10 gradually approach zero at remote locations; e.g., the zero-bias conductance in curve  $c$  of Fig. 1, for  $r = 2000 \text{ \AA}$ , is nil.

Figure 11 shows two three-dimensional views of the STM conductance near a vortex calculated from the theory presented here.  $g(E, x)$ , where  $E = eV$ , was evaluated from Eq. (26) and is plotted versus  $E$  and  $x$ , the linear coordinate along a line through the vortex center. The total range (along  $x$ ) is  $308 \text{ \AA}$ , i.e.,  $4R$ . An experimental view of this type was presented in Fig. 4 of Ref. 4 but included a range of  $1000 \text{ \AA}$ . Finally, we note that an alternative approach based on the Bogoliubov-de Gennes equations<sup>19</sup> has been attempted.<sup>20</sup> The formidable computational effort required in solving (numerically) the Bogoliubov-de Gennes equations led us to seek a simpler (but perhaps less profound) approach. In the form ordinarily used, the Bogoliubov-de Gennes equa-

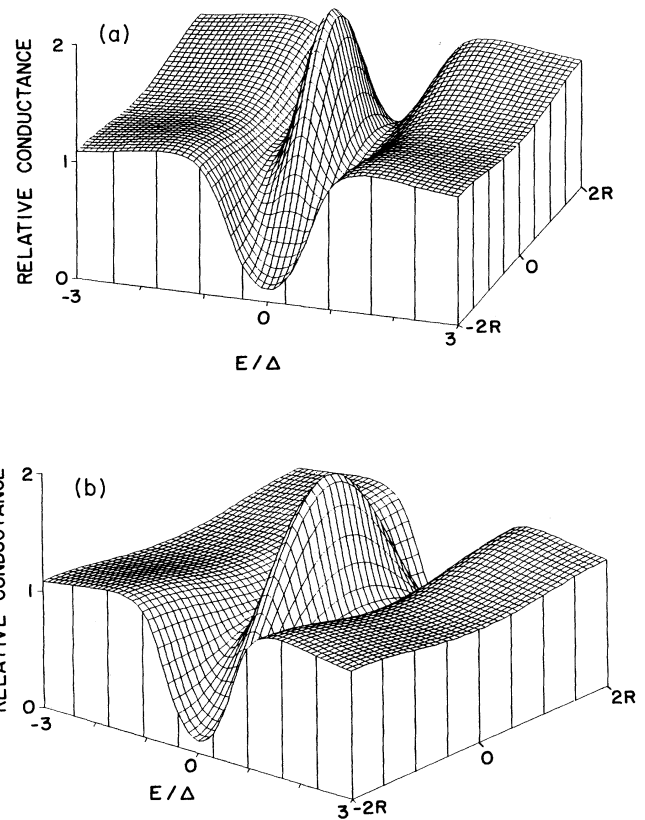


FIG. 11. Two three-dimensional perspectives of the tunneling conductance vs bias voltage and STM location relative to the center of the vortex.

tions assume a local ( $\delta$ -function) pairing potential rather than a nonlocal kernel of range  $\xi_0$  as is found, for instance, in the Eliashberg equations. Consequently we do not know whether the alternative approaches are equivalent.

#### ACKNOWLEDGMENTS

We are grateful to Paul Muzikar for numerous discussions. We are indebted to the National Science Foundation, Condensed-Matter Theory section for financial support. One of us (L.L.D.) would like to thank the Purdue Research Foundation for partial support.

<sup>1</sup>C. Caroli and J. Matricon, *Phys. Kondens. Mater.* **3**, 380 (1965); C. Caroli, P. G. de Gennes, and J. Matricon, *Phys. Lett.* **9**, 307 (1964); M. Cyrot, *Phys. Kondens. Mater.* **3**, 374 (1964).

<sup>2</sup>R. Leadon and H. Suhl, *Phys. Rev.* **165**, 596 (1968).

<sup>3</sup>R. Watts-Tobin, L. Kramer, and W. Pesch, *J. Low Temp. Phys.* **17**, 71 (1974).

<sup>4</sup>H. F. Hess, R. B. Robinson, R. C. Dynes, J. M. Valles, Jr., and J. V. Waszicak, *Phys. Rev. Lett.* **62**, 214 (1989).

<sup>5</sup>A. W. Overhauser and L. L. Daemen, *Phys. Rev. Lett.* **62**, 1691 (1989).

<sup>6</sup>V. Weisskopf and E. Wigner, *Z. Phys.* **63**, 54 (1930); see also E. Arnow and W. Heitler, *Proc. R. Soc. (London), Ser. A* **220**, 290 (1953).

<sup>7</sup>C. Cohen-Tenoudji, B. Diu, F. Laloe, *Quantum Mechanics II*, (Wiley, New York, 1977), Chap. XIII, p. 1343; see also E. Merzbacher, *Quantum Mechanics*, (Wiley, New York, 1970), Chap. 19, p. 481.

- <sup>8</sup>E. C. McIrvine and A. W. Overhauser, *Phys. Rev.* **115**, 1531 (1959); E. C. McIrvine, *ibid.* **115**, 1537 (1969).
- <sup>9</sup>J. Bardeen, L. N. Cooper, and J. R. Schrieffer, *Phys. Rev.* **108**, 1175 (1957).
- <sup>10</sup>M. H. Cohen, L. M. Falicov, and J. C. Phillips, *Phys. Rev.* **108**, 1175 (1957).
- <sup>11</sup>J. M. Ziman, *Elements of Advanced Quantum Mechanics* (Cambridge University Press, Cambridge, 1969), Chap. 3, p. 53; M. L. Goldberger and K. M. Watson, *Collision Theory* (Wiley, New York, 1964), Chap. 8, p. 424.
- <sup>12</sup>E. U. Condon and G. H. Shortley, *The Theory of Atomic Spectra* (Cambridge University Press, Cambridge, 1959), Chap. II, p. 37.
- <sup>13</sup>See, for example, A. Böhm, M. Gadella, and G. Bruce Mainland, *Am. J. Phys.* (to be published); A. Böhm, *Quantum Mechanics* (Springer-Verlag, New York, 1979), Chap. XXI.
- <sup>14</sup>R. E. Prange and L. P. Kadanoff, *Phys. Rev.* **134**, A566 (1964), Eqs. (47) and (48c).
- <sup>15</sup>Kazumi Maki, in *Superconductivity*, edited by R. D. Parks (Dekker, New York, 1969), Vol. 2, p. 1035, see especially the Appendix.
- <sup>16</sup>John W. Wilkins, *Observable Many-Body Effects in Metals* (Nordita, Copenhagen, 1986), Chap. II.
- <sup>17</sup>E. L. Wolf, *Principles of Electron Tunneling Spectroscopy* (Oxford University Press, New York, 1985), Eq. (3.2), p. 81.
- <sup>18</sup>P. de Trey, S. Gygax, and J. P. Jan, *J. Low Temp. Phys.* **11**, 421 (1973).
- <sup>19</sup>P. G. de Gennes, *Superconductivity of Metals and Alloys* (Benjamin, New York, 1966), Chap. 5.
- <sup>20</sup>J. D. Shore, Ming Huang, A. T. Dorsey, and J. P. Sethna, *Phys. Rev. Lett.* **62**, 3089 (1989).